Desalination and Water Treatment
www.deswater.com

doi: 10.5004/dwt.2018.21918

112 (2018) 19–33
April

Fluoride removal from water by lime-sludge waste

Rajkamal Mohan, Anup Jyoti Bora, Robin K. Dutta*

Department of Chemical Sciences, Tezpur University, Tezpur 784028, Assam, India, Tel. +91 3712 265055, +91 9957 077808; Fax: +91 3712 267005; emails: robind@tezu.ernet.in (R.K. Dutta), Tel. +918876166571; email: rkmohan@tezu.ernet.in (R. Mohan), Tel. +917399920194; email: ajbora1@tezu.ernet.in (A.J. Bora)

Received 19 September 2017; Accepted 5 January 2018

ABSTRACT

The potential application of lime-sludge waste (LSW) from paper mills in removal of excess fluoride from water has been studied. Strings of batch experiments were carried out to assess the fluoride removal ability of dried micrometer-sized LSW in presence of phosphoric acid (PA) by varying operational parameters, viz., initial fluoride concentration, initial PA concentrations, contact time and adsorbent dose. The adsorption data fitted well to Freundlich model and pseudo-second-order kinetics. The mechanism of removal has been suggested as a combination of precipitation of fluorite and fluorapatite (FAP), and adsorption by hydroxyapatite (HAP). Fluoride was found to be reduced from initial 10 mg/L to less than 1 mg/L in 30 min. The maximum fluoride adsorption capacity of LSW was found to be 0.943 mg g^{-1}. The quality parameters of the treated water remain within WHO guidelines and the exhausted used LSW very well passes the toxicity characteristic leaching procedure test of the US-EPA. The study shows LSW, a waste material, as a potential sorbent for remediation of fluoride contaminated water.

Keywords: Fluoride removal; Lime-sludge waste; Phosphoric acid; Hydroxyapatite

1. Introduction

The presence of fluoride in drinking water up to a certain limit is beneficial to formation and maintenance of healthy bones and teeth [1], while its excess intake abets dental and skeletal fluorosis in addition to formation of contusion in various body organs such as pituitary glands, thyroid and liver [2]. The World Health Organisation (WHO) suggests a guideline value of 1.5 mg/L for fluoride in drinking water [3]. In many parts of the world including countries such as China, India, Japan, Jordan, Brazil, Tanzania and Pakistan, fluoride level in groundwater exceeds the guideline value making fluorosis a grave health issue [4,5]. While fluoride-bearing rocks such as sellaite (MgF_2), fluorspar (CaF_2), cryolite (Na_3AlF_6) are the main source of fluoride in ground water [6], industries such as aluminium industry, steel production plants, etc., also contaminate surface water and groundwater with excess fluoride [7]. Therefore, defluoridation of fluoride-contaminated groundwater and industrial effluent is very much essential to dispose of this menace.

The methods of fluoride removal are based on coagulation/precipitation [8], ion exchange [9], reverse osmosis [10], electrocoagulation [11], nanofiltration [12] and adsorption [13]. Of all these techniques, some suffers drawbacks such as low efficiency due to presence of competitive ions, high cost, production of huge amount of sludge, etc. Adsorption is one of the most widely used principle due to its selectivity, higher efficiency, lower operating cost, easy handling nature, ability to generate lesser quantity of sludge and regeneration ability of spent adsorbent [14]. Some of the well-known geomaterials such as limestone [15–19], magnesite [20], gypsum [20], bauxite [21], pumice stone [22], diatomite and ignimbrite material [23] were demonstrated as good fluoride adsorbents. Low-cost materials such as tree bark, fungi, wood charcoal, saw dust and other waste materials were also tried [24,25].

Adsorptions of fluoride on waste carbon slurry [26] and waste mud from Cu–Zn mining industry [27] have been

* Corresponding author.

reported. Lime-sludge waste (LSW) is a major muddy waste product of paper mills with no economically feasible method for disposal or reuse as is evident from a picture of the menace created by its dumping (supporting information 1). On the other hand, fluoride contamination of groundwater is also creating another menace in nearby vast areas of Assam and its neighbourhood [28–30]. LSW, which mainly consists of calcium carbonate [31], is expected to remove fluoride similar to other lime materials.

Therefore, in order to explore the possibility of utilizing this waste in remediation of fluoride contaminated water, we have carried out a study on adsorption behaviour of fluoride from synthetic water by LSW in presence of phosphoric acid (PA). The fluoride removal by LSW in presence of PA has been evaluated using batch sorption experiments as a function of initial fluoride concentration ($[F^-]_0$), initial PA concentration ($[PA]_0$), contact time and sorbent dose. The mechanism of fluoride removal was addressed using PHREEQ model [15,32] and characterization of the products using various experimental techniques. The safety and environmental aspects have also been addressed.

2. Materials and methods

2.1. Materials

LSW was collected in a plastic bag from the dump site of the paper mill of Hindustan Paper Corporation Limited, Jagiroad, Assam, India. The LSW sample was dried at 120°C in an oven for 24 h, pulverised and the <200 μm particle size powder was stored in airtight plastic containers. GR grade sodium fluoride (NaF) from Merck (Mumbai) and 85% w/v PA from Rankem (Ankleshwar, Gujarat) were used as such. Fluoride stock solution of 1,000 mg/L concentration was prepared by dissolving NaF in millipore water. The test solutions were prepared by diluting the stock solution with tap water with appropriate adjustment of fluoride and PA concentrations. The quality parameters of the tap water can be seen in Table 1 as parameters before treatment.

Table 1
Water quality parameters before and after treatment using LSW with $[F^-]_0$ = 5 mg/L, $[PA]_0$ = 0.05 M, adsorbent dose = 1.5 g/100 mL

Parameter in mg/L except for pH	WHO guideline value	Before treatment	After treatment
pH	6.50–8.50[a]	7.47	6.95
Dissolved solid	600	130	432
Suspended solid	NS	10	48
Total alkalinity as $CaCO_3$	200	83	135
Total hardness as $CaCO_3$	200	80	123
Sulphate	500	6.3	6.2
Phosphate	NS	0.70	1.82
Nitrate	50	0.55	0.46
Cadmium	0.003	ND	ND
Calcium	50	2.50	38.4
Mercury	0.001	ND	ND
Chromium	0.05	ND	0.003
Cobalt	NS	ND	ND
Copper	2.0	1.00	0.10
Arsenic	0.01	ND	ND
Lead	0.01	ND	ND
Magnesium	NS	2.4	18.2
Manganese	0.40	0.10	0.12
Zinc	3.0	0.09	0.02
Sodium	200	60.6	66.9
Potassium	NS	1.07	3.06
Iron	0.30	0.34	0.10

NS, not specified; ND, not detectable.
[a]Acceptable range for drinking.

2.2. Sorption studies

All sorption experiments were conducted in batch mode at room temperature (300 ± 2 K) in 250 mL polycarbonate bottles, where a predetermined amount of LSW was added to 100 mL of fluoride containing water pre-acidified with PA. A thermostated shaker was used to shake this mixture at a speed of 140 rpm for a predetermined time interval. Consequently, the suspension was filtered through Whatman 42 filter paper and the leftover fluoride concentrations in the water were measured. The experiments were repeated at least thrice in order to check reproducibility. The thermodynamic parameters of sorption were established by conducting the experiments at 300, 308, 313, 318 and 323 (±1) K.

The defluoridation capacity of LSW at time t (q_t) and at equilibrium (q_e) was determined by using Eqs. (1) and (2), respectively [33]:

$$q_t = \frac{(C_o - C_t)V}{m} \quad (1)$$

$$q_e = \frac{(C_o - C_e)V}{m} \quad (2)$$

where C_o, C_t and C_e are the initial fluoride concentration, the fluoride concentration at time t and the equilibrium fluoride concentration, respectively; V is the volume of the solution in L and m is the mass of the sorbent taken in g.

2.3. Desorption analysis

Desorption from the loaded LSW was evaluated using a collection of 40 mg/L fluoride solutions of 100 mL, pre-acidified with 0.05 M PA [14,34]. This solution was mixed with 1.5 g of sorbent under the following experimental conditions: initial pH = 1.85, temperature = 300 K, contact time = 12 h and agitation speed = 140 rpm. The equilibrium solution was emptied and the fluoride-loaded sorbent was then added to a set of 20 mL distilled water with varying pH ranging from 3 to 12 adjusted with 0.1 M NaOH and

0.1 M HCl. Desorption was studied under the experimental conditions: temperature = 300 K, contact time = 3 h and agitation speed = 140 rpm. The concentrations of fluoride desorbed into the solutions were then measured.

2.4. Instrumental analysis

The concentration of fluoride in the solutions was measured using a Multiparameter Kit (model: Orion Versa star pH-ISE-Cond-RDO-DO), which was attached to an Orion fluoride ion-selective electrode (ISE) probe. The pH was determined using an Orion Multiparameter Kit (Orion 5 Star pH-ISE-Cond-DO Benchtop) using a pH electrode. Total ionic strength adjustment buffer III supplied by Orion Ionplus® was used to decomplex fluoride ions. The metal ions in water before and after treatment were determined using atomic absorption spectrophotometer (iCE 3000 series, Thermo Fisher Scientific, USA). The existence of calcium, sodium and potassium ion in the samples was analysed by a flame photometer (Flame Photometer 128, Systronics, India). The Fourier transform infrared (FTIR) spectra were recorded on a Frontier MIR FIR spectrometer (PerkinElmer, USA) in KBr medium at room temperature in the region 4,000–400 cm^{-1}. The X-ray diffraction (XRD) data were collected on a Miniflex X-ray diffractometer (Rigaku, Japan) with Cu-Kα radiation (λ = 0.154 nm) at 30 kV and 15 mA using a scanning rate of 0.05°/s in 2θ ranges from 10° to 70°. The surface morphology of the samples was obtained from a SEM (model JSM-6390LV, JEOL, Japan) with an energy dispersive X-ray (EDX) attached.

3. Results and discussion

3.1. Characterisation of LSW

3.1.1. FTIR analysis

The major characteristic vibrational bands of LSW, before use, were observed at 2,513; 1,431; 873; 712 and 457 cm^{-1} which correlate with the plane bending vibration of carbonate (Fig. 1(A)) [33,35]. The spectrum after fluoride sorption by LSW showed broadening of band at 3,486 cm^{-1}, which may be taken as an indication of electrostatic adsorption between the sorbent and fluoride [36]. The intensities of the carbonate peaks were found to decrease after fluoride sorption which may be due to incorporation of PO_4^{3-} ions replacing CO_3^{2-} ions. Notable peaks at 1,121; 1,067; 986 and 577 cm^{-1} after use indicates formation of hydroxyapatite (HAP) [33,34,37]. Peaks at 3,547; 1,651; 1,213; 1,121; 1,067; 986; 662; 577 and 526 cm^{-1} indicates the formation of brushite ($CaHPO_4.2H_2O$), which may form at low pH prevailing in the initial stage with high $[PA]_0$ [38]. A low intensity peak of Ca–F stretching band at 793 cm^{-1} can be attributed to the presence of small quantity of CaF_2 [39]. Absence of any peak at 840 cm^{-1} in the spectrum of LSW after fluoride sorption indicates absence of Si–F bond [40]. Thus, IR spectra suggest that LSW, after fluoride removal, contains mainly calcium carbonate along with some calcium phosphate in the form of HAP and small quantities of brushite and fluorite.

3.1.2. XRD analysis

In the XRD spectra of unused LSW (Fig. 1(B)), prominent peaks at 2θ = 22.9°, 29.3° (strong), 35.9°, 39.3°, 43.1°, 47.4° and 48.4° (JCPDS card number 72-1937) provides evidence of calcite polymorph of calcium carbonate [37]. The XRD of the sorbent, after fluoride loading, showed majority of these peaks but with some changes in relative intensities. The peaks with considerable intensities at 2θ = 30.8°, 35.4°, 39.7°, 41.7°, 49.2°, 50.4°, 53.7° and 55.1° (JCPDS card number 74-0565) clearly suggest the formation of HAP in the sorbent [33,34,37,41,42]. Sizeable peaks at 2θ = 11.9°, 22.9° (JCPDS card number 72-0713) indicate the formation of brushite [38]. Presence of fluorapatite (FAP) can be inferred from the small peaks at 31.5°, 42.3° and 60.7° (JCPDS card number 83-0557) [41,42]. Formation of FAP may be due to strong affinity of HAP towards adsorption of fluoride [34]. There is precipitation of FAP also to a small extent as the solubility product of FAP is much smaller than that of HAP; however, a dominant presence of OH^- ions is expected to suppress the precipitation

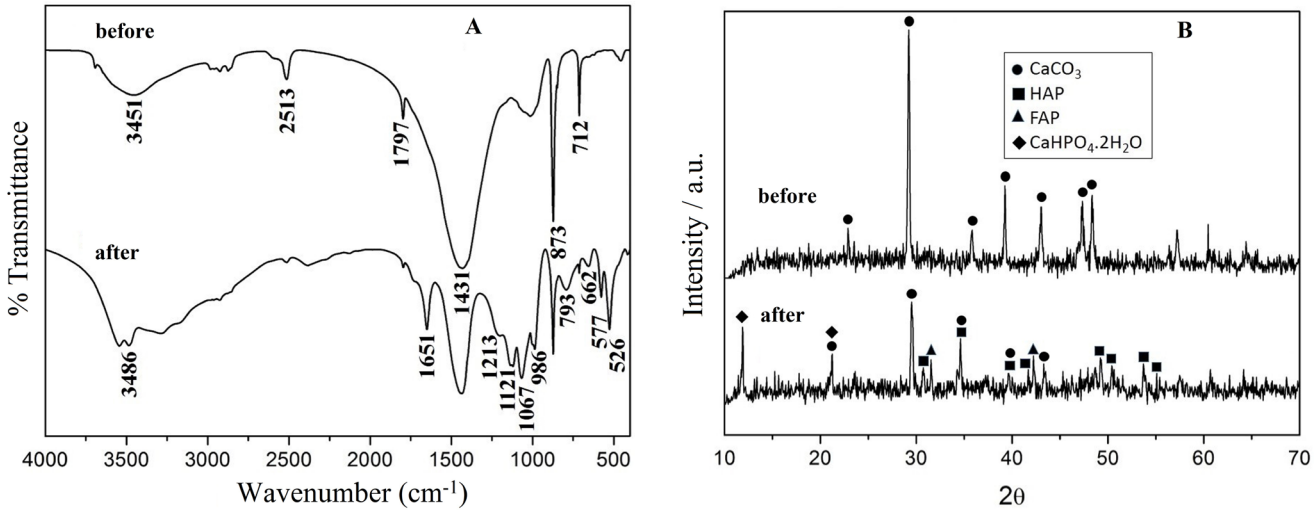

Fig. 1. FTIR spectra (A) and XRD patterns (B) of LSW, before and after fluoride sorption in presence of PA.

of FAP [43]. Absence of any significant peak at 46.9° indicates the absence of significant quantity of fluorite (CaF_2) in the sorbent after use [44]. Thus, with the help of these evidences it can be proposed that in the present process, fluoride removal is due to adsorption by HAP, which forms FAP after sorption of fluoride through ion exchange.

3.1.3. SEM–EDX analysis

From the SEM micrograph of fresh LSW, it appears that the particles are randomly shaped and appears to be <10 μm in size (Fig. 2(A)). The EDX spectrum of fresh LSW revealed the presence of high concentration of Ca, C and O along with small amount of Na, Mg and Si. None of the heavy metals were found in excess in the adsorbent (Fig. 2(A)). The elemental composition of LSW before and after treatment has been shown in Table 2. However, in the SEM micrograph of fluoride loaded LSW, cylindrical rods were observed (Fig. 2(B)) which can be attributed to the formation of HAP [45]. Besides, EDX spectrum of fluoride loaded LSW showed loss in the amount of Ca after treatment, which may be due to disintegration of LSW after reaction with acidic fluoride water. This is confirmed by the corresponding increase in the amount of Ca in the treated water [17]. The percentage of fluoride in LSW after treatment was found to increase as expected due to adsorption of fluoride by HAP and precipitation as fluorite. On the other hand, amount of phosphorus and oxygen increased due to the formation of HAP.

3.2. Characterisation of water before and after treatment

The relevant water quality parameters of the treated water were determined before and after treatment by LSW using standard methods [46] and are presented in Table 1 along with the guidelines values of WHO [3]. Although our initial objective was to treat industrial effluent with high fluoride content and believed that the LSW should be used as such, it has been interesting to see that the water quality parameters after treatment indeed fulfilled the prescribed WHO guideline values for drinking purposes. Although there is some spike in the values of some parameters after treatment, they were within the WHO guideline values. The increase in the concentration of Mg, Na, K and Ca in the treated water has led to spike in the concentration of dissolved solid in the treated water. Similarly, an increase in concentration of suspended solid after treatment indicates that some amount of undissolved particles remains in the treated water after filtration using Whatman 42 filter paper. Since LSW is primarily composed of $CaCO_3$, there is an increase in the amount of carbonate ions in the treated water due to which the concentration of total alkalinity as $CaCO_3$ has increased. Moreover, the concentration of Ca^{2+} and PO_4^{3-} which are the two primary constituents present in the materials used in the current method apart from Mg^{2+} increased in the treated water but persisted within the WHO guideline values owing to the very low solubility product of calcium phosphates. Due to this reason, the concentration of total hardness as $CaCO_3$ has also increased.

Table 2
Elemental composition of LSW before and after fluoride loading in presence of PA as obtained from SEM–EDX

Elements	Before use		After use with PA	
	Weight%	Atomic%	Weight%	Atomic%
C	8.39	14.10	9.48	15.47
O	50.96	64.30	52.76	64.19
F	0	0	4.77	5.03
Na	0.72	0.63	0.15	0.12
Mg	1.20	1.00	0.35	0.28
Al	0.52	0.39	0.43	0.31
Si	2.33	1.67	2.74	1.91
P	0	0	9.37	5.93
Ca	34.85	17.55	18.40	6.25
Ti	0.10	0.04	0.10	0.04
Cr	0.04	0.01	0.04	0.02
Fe	0.12	0.04	0.44	0.15
Cu	0.65	0.21	0.38	0.12
Zn	0.11	0.03	0.59	0.18

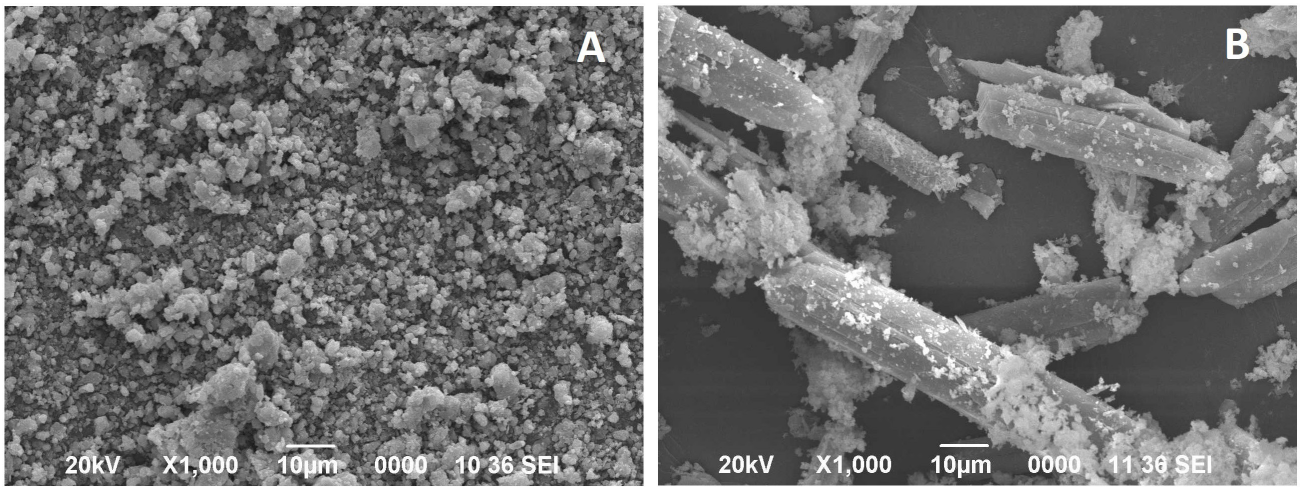

Fig. 2. SEM images of LSW (A) before and (B) after fluoride sorption in presence of PA.

3.3. Fluoride sorption by LSW

3.3.1. Effect of contact time and initial fluoride concentration

The removal of fluoride by LSW with varying $[F^-]_0$ of 3, 5, 7, 10 and 20 mg/L as a function of contact time with fixed sorbent dose of 1.5 g/100 mL, $[PA]_0$ of 0.05 M and a shaking speed of 140 rpm are shown in Fig. 3(A). Fluoride removal was achieved from initial 10 mg/L to less than 1 mg/L in 30 min. The initially rapid fluoride removal slowed down gradually to reach equilibrium in about 30 min as expected. Such dependence of fluoride removal on initial $[F^-]_0$ and contact time was reported for other adsorbents [36,41,47]. The final $[F^-]$ in the treated water decreased gradually from 1.46 to 0.40 mg/L on decreasing the $[F^-]_0$ from 20 to 3 mg/L which shows that LSW in combination with PA is capable of removing fluoride to below the WHO guideline value of 1.5 mg/L for fluoride in drinking water. The percentage fluoride removal increased from 87% to 92.5% with increase in $[F^-]_0$ from 3 to 20 mg/L.

The removal of fluoride by LSW in presence of PA achieved equilibrium in reasonably less contact time compared with 3 h taken by limestone in presence of PA reported earlier [37,48]. The shorter time taken with LSW may be due to easier dissolution of $CaCO_3$ of LSW than that of limestone. The initial rapid fluoride removal slowing down to cease after 30 min may be due to initial dominance by precipitation and continuation of adsorption up to about 30 min as precipitation is expected to be complete at much shorter time than adsorption [18]. The time required to achieve equilibrium was found to be independent of initial fluoride concentration. The pH of the fluoride containing pre-acidified water before treatment was found to be around 1.85. However, the final pH of the water after fluoride adsorption in these experiments was found to be in the range of 5.19–6.75, which is within the acceptable range for drinking.

3.3.2. Effect of initial PA

The fluoride removal by LSW in presence of varying $[PA]_0$ of 0.01, 0.03, 0.05, 0.07 and 0.10 M with fixed $[F^-]_0$ of 5 mg/L, sorbent dose of 1.5 g/100 mL and a shaking speed of 140 rpm is shown in Fig. 3(B). The fluoride removal increased with increasing $[PA]_0$, which may be attributed to increased precipitation of CaF_2 and FAP and increased adsorption of fluoride by newly formed calcium phosphates such as HAP from the reaction of LSW with PA and F^- [33]. The pH was found to increase rapidly in the first 30 min, which then continued to increase slowly until levelling off in about an hour

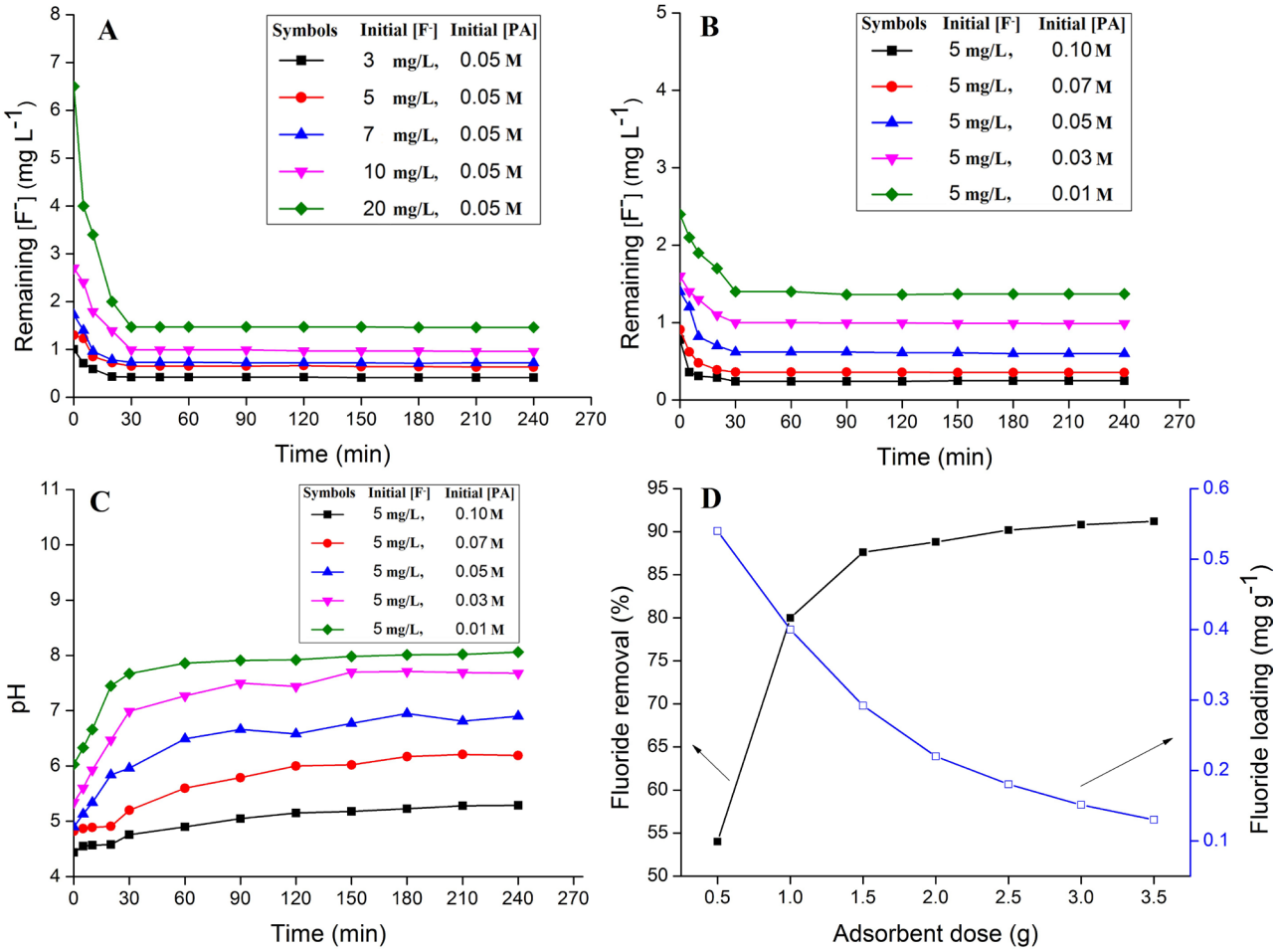

Fig. 3. Effects of (A) contact time and initial fluoride concentration, (B) contact time and initial PA concentration, (C) contact time and initial PA concentration on pH and (D) dosage of LSW on fluoride removal at 300 K. Error limit in $[F^-] = \pm 0.01$ mg L^{-1}.

(Fig. 3(C)). This indicates a continuation of the neutralization of PA by $CaCO_3$ even after completion of the fluoride adsorption. The initial pH of the untreated fluoride containing pre-acidified water was found to be in the range of 1.81 to 2.38 when $[PA]_0$ was varied from 0.10 to 0.01 M. However, the final pH of the treated water was found to be in the range of 5.0–8.0 on decreasing the $[PA]_0$ from 0.10 to 0.01 M.

With the initial pH below 3.5 of the untreated water, there is a possibility of formation of HF and subsequently hexafluorosilicic acid $(H_3O)_2[SiF_6]$, which may influence the removal of fluoride from water. To understand the effect, we conducted an experiment in polycarbonate bottles where LSW and pure SiO_2 (0.1–0.3 mm particle size) in the ratios of 1:0, 1:1 and 0:1 were used to remove fluoride from water pre-acidified with PA under the following experimental conditions: initial pH: 1.85, temperature = 300 K, $[F]_0$ = 10 mg/L, $[PA]_0$ = 0.05 M, adsorbent dose: 1.5 g/100 mL, contact time = 90 min and agitation speed = 140 rpm. It was found that pure SiO_2 was able to remove only a small amount of fluoride (final [F] = 7.8 mg/L) (supporting information 2) whereas, fluoride removal was much more with LSW. The final [F] was 1.8 and 0.99 mg/L with 1:1 ratio of LSW and sand, and LSW alone, respectively. This indicates a dominance of $CaCO_3$ in fluoride removal over silica in case of LSW, as silica is present in a much smaller percentage compared with $CaCO_3$ in LSW (Table 2). Also, $CaCO_3$ is a much stronger base than SiO_2 leading to rapid neutralisation of the acid by $CaCO_3$, thus raising the pH rapidly to above 4.5 in less than a minute (Fig. 3(C)). The final pH of the treated water was found to be 6.39 with LSW as the sole adsorbent, while it remained nearly unchanged (pH = 1.99) when pure SiO_2 was used. Moreover, no characteristic peak in FTIR and P-XRD was observed to support the formation of any Si–F bond.

3.3.3. Adsorption kinetics

The kinetics of fluoride sorption by LSW was investigated to determine residence time for completion of sorption and selecting optimum operating conditions for full-scale batch process. The adsorption data were evaluated using pseudo-first-order, pseudo-second-order, intra-particle diffusion and Elovich model with $[F^-]_0$ ranging from 3 to 20 mg/L, sorbent dose of 1.5 g/100 mL and $[PA]_0$ of 0.05 M. The adsorption reached equilibrium within 60 min.

The pseudo-second-order model can be expressed as [49]:

$$\frac{t}{q_t} = \frac{t}{q_e} + \left(\frac{1}{k_2}\right)\left(\frac{1}{q_e^2}\right) \tag{3}$$

where k_2 is pseudo-second-order rate constant in g mg^{-1} min^{-1}. The values of q_e and k_2 presented in Table 3 are obtained from the slope and intercept of the plot of t/q_t vs. time t. The r^2 values close to unity suggest that pseudo-second-order model fits very well with this adsorption process. Fig. 4 shows the plot of q_t versus t. The kinetics of adsorption of fluoride on LSW did not fit well to the pseudo-first-order, intra-particle diffusion and Elovich models. Details of these models along with the kinetic parameters can be seen in supporting information 3. Based on the r^2 values of the kinetic models it can be established that, for the present adsorption process, the kinetic models fits in the following order: pseudo-second-order > Elovich > pseudo-first-order > intra-particle diffusion model.

Table 3
Kinetic parameters obtained for different kinetic models from fluoride adsorption on LSW at different $[F^-]_0$ with a sorbent dose of 1.5 g/100 mL and $[PA]_0$ of 0.05 M at 300 (±1) K

Parameters	$[F^-]_0$ (mg/L)				
	3	5	7	10	20
Pseudo-first-order model					
k_1 (min^{-1})	0.1295	0.1404	0.1224	0.1484	0.2049
q_e, cal (mg g^{-1})	0.0401	0.0771	0.0738	0.2785	0.9796
q_e, exp (mg g^{-1})	0.1726	0.291	0.4193	0.6020	1.2360
r^2	0.9514	0.9743	0.9837	0.8689	0.8399
Pseudo-second-order model					
k_2 (g mg^{-1} min^{-1})	2.2666	1.4948	0.9320	0.7342	0.3558
q_e, cal (mg g^{-1})	0.1733	0.2910	0.4197	0.6045	1.2390
q_e, exp (mg g^{-1})	0.1726	0.291	0.4193	0.6020	1.2360
r^2	0.9999	0.9999	0.9999	0.9999	0.9999
Intra-particle diffusion model					
k_i (g mg^{-1} $min^{-1/2}$)	0.0065	0.0113	0.0131	0.0280	0.0548
r^2	0.8813	0.7845	0.7844	0.9539	0.9774
Elovich model					
A (mg g^{-1} min^{-1})	0.7119	1.207	1.4206	1.6758	1.8213
$1/B$ (mg g^{-1})	0.0120	0.0213	0.0249	0.0512	0.0979
r^2	0.9521	0.8980	0.8983	0.9878	0.9524

3.3.4. Adsorption isotherm

To assess the adsorption limit of LSW and further understand the adsorption mechanism, the Freundlich, Langmuir, Dubinin–Radushkevich (D–R) and Temkin isotherm plots were studied using water with $[F^-]_0$ in the range of 3–20 mg/L, a sorbent dose of 1.5 g/100 mL and $[PA]_0$ of 0.05 M at 300 (±1) K. The model equation of Freundlich isotherm in the linear form is presented below [33]:

$$\ln q_e = \ln K_F + \frac{1}{n}\ln C_e \tag{4}$$

where C_e and q_e are the equilibrium fluoride concentration in mg/L and adsorption capacity of sorbent in mg g^{-1} at equilibrium, respectively. K_F in mg g^{-1} and n are Freundlich isotherm constants associated to adsorption capacity and adsorption intensity, respectively. The values of n and K_F are obtained from the slope and intercept of the plot of ln q_e vs. ln C_e and listed in Table 4. With r^2 of 0.9890 and $1/n$ between 0.1 and 1.0, the Freundlich isotherm can be employed to describe the fluoride sorption process using LSW [50]. Fig. 5 shows the plot of q_e versus C_e. Details of the Langmuir, D–R and Temkin isotherms can be found in supporting information 4. The Langmuir adsorption capacity was found to be 0.943 mg g^{-1} (Table 4). From the analyses of the above isotherms including the r^2

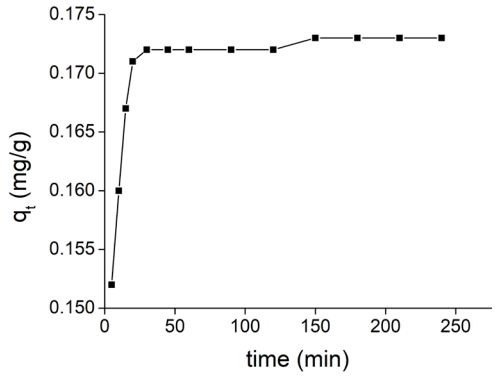

Fig. 4. Plot of q_t vs. t for fluoride sorption on LSW (conditions: $[F^-]_0$: 3 in mg/L, $[PA]_0$: 0.05 M, equilibrium pH: 6.75, temperature: 300 (±1) K, sorbent dose 1.5 g/100 mL).

Table 4
Isotherm data for adsorption of fluoride on LSW

Isotherm parameters	
Freundlich	
K_F (mg g^{-1})	0.664
1/n	0.861
r^2	0.989
Langmuir	
Q_o (mg g^{-1})	0.943
b (L mg^{-1})	1.344
r^2	0.8651
Temkin	
A_T (L/g)	2.5183
B_T	0.8322
r^2	0.8543
Dubinin–Radushkevich	
B_D ($mol^2\,kJ^{-2}$)	0.197
Q_D (mg g^{-1})	2.743
E (kJ mol^{-1})	1.593
r^2	0.896

values, it can be established that the isotherms fit with the fluoride adsorption by LSW in the following order: Freundlich > D–R > Langmuir > Temkin isotherm.

3.3.5. Effect of sorbent dose

The dose of LSW was varied from 0.5 to 3.5 g/100 mL with fixed $[F^-]_0$ of 5 mg/L, $[PA]_0$ of 0.05 M and a shaking speed of 140 rpm to see the effect of the adsorbent dose on fluoride removal at equilibrium. The contact time was chosen to be 90 min to allow the system to attain complete equilibrium (Fig. 3(D)). It was observed that 54% of fluoride was removed, after equilibrium, with a sorbent dose of 0.5 g/100 mL which gradually increased to 92% with 3.5 g/100 mL of adsorbent dose and was levelled off above that dose. As expected, there was a steady decline in the quantity of fluoride adsorbed per gram of the sorbent with increase in the dose.

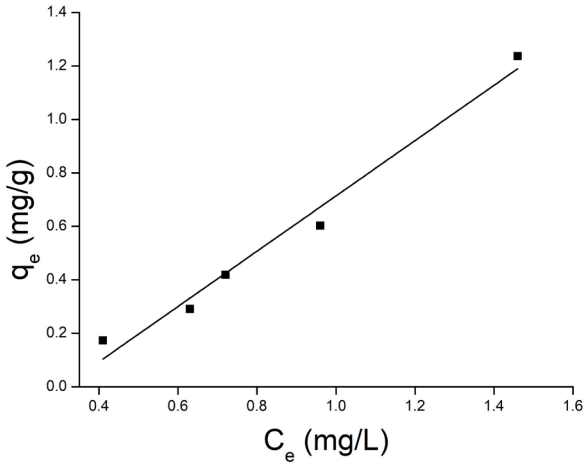

Fig. 5. Adsorption isotherm of fluoride sorption on LSW at varying $[F^-]_0$ of 3, 5, 7, 10, 20 mg/L (conditions: $[PA]_0$: 0.05 M, equilibrium pH range: 5.19–6.75, temperature: 300 (±1) K, contact time 90 min, sorbent dose 1.5 g/100 mL).

3.4. Fluoride desorption

Fluoride desorption from the sorbent was observed to be low in neutral and acidic conditions, yet expanded quickly from 8% at pH 7 to 90% at pH 12. Fig. 6(B) shows the percentage of fluoride desorption from the sorbent as a function of solution pH. The higher desorption in alkaline condition suggests exchange of F^- ions with OH^- ions [14,34].

3.5. Mechanism of fluoride removal by LSW

3.5.1. PHREEQ analysis

To throw some light on the mechanism of fluoride removal by LSW in presence of PA, we have analysed the equilibrium of the process by PHREEQ model. PHREEQ is an equilibrium-modelling program capable of simulating chemical reactions and transport processes in natural and polluted water. The "llnl.dat" database was employed in this study due to its comprehensiveness. Since $CaCO_3$ is the major constituent of LSW, PHREEQ modelling was done using $CaCO_3$ for LSW and NaF for $[F^-]_0$. With $[F^-]_0$ = 5 mg/L, $CaCO_3$ = 15 g/L, $[PA]_0$ = 0.1 M and atmospheric pCO_2 ~$10^{-3.5}$ atm (0.03%) the program predicted a model pH = 5.028 and very low $[F]_{eq}$ (<10^{-10} moles) of the treated water. This model pH is almost identical to the experimental pH (Fig. 3(C), black line). However the predicted [F] is much lower than the experimental value (Fig. 3(B), black line), which is most likely due to limitation of the fluoride ISE used for analysis. The model also predicted formation of FAP (2.632 × 10^{-4} moles) and HAP (2.708 × 10^{-2} moles) in the system. These results confirm the ability of LSW to remove fluoride from water.

3.5.2. Schematic mechanism

Based on the above analysis, the following reactions have been proposed to take place in the process of fluoride removal by LSW in presence of PA:

$$CaCO_3(s) + 2H_3PO_4 \rightarrow Ca^{2+} + 2H_2PO_4^- + CO_2 + H_2O \quad (5)$$

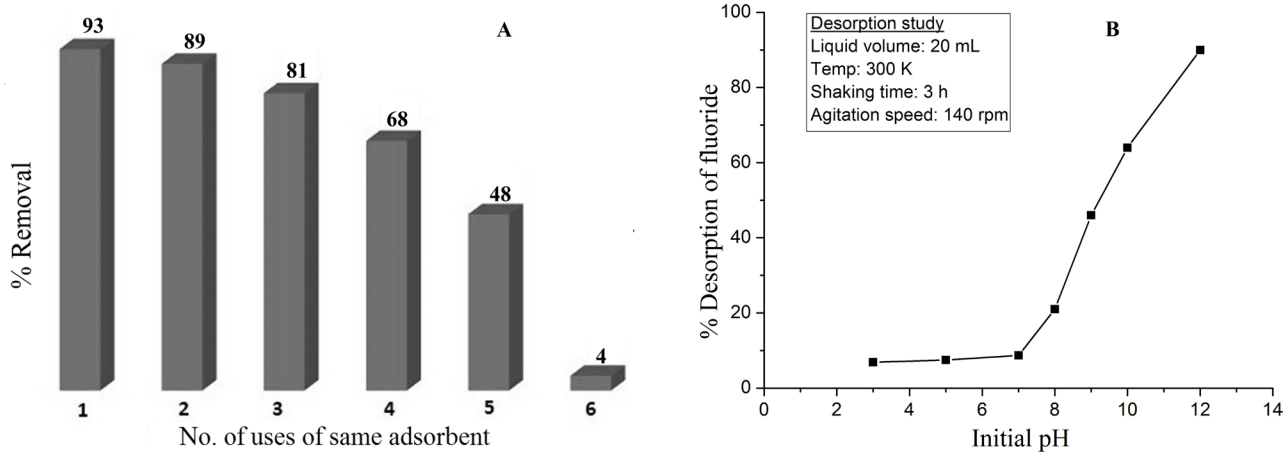

Fig. 6. Reusability of the sorbent (A) and desorption study from fluoride-loaded LSW (B) at different pH.

$$CaCO_3(s) + 2H_2PO_4^- \rightarrow Ca^{2+} + 2HPO_4^{2-} + CO_2 + H_2O \quad (6)$$

$$Ca^{2+} + F^- \rightarrow CaF_2(s)\downarrow \quad (7)$$

$$Ca^{2+} + H_3PO_4 + 2H_2O \rightarrow CaHPO_4.2H_2O(s)\downarrow + 2H^+ \quad (8)$$

$$5Ca^{2+} + 3HPO_4^{2-} + 3OH^- + F^- \rightarrow Ca_5F(PO_4)_3(s)\downarrow + 3H_2O \quad (9)$$

$$5Ca^{2+} + 3HPO_4^{2-} + 4OH^- \rightarrow Ca_5(OH)(PO_4)_3(s)\downarrow + 3H_2O \quad (10)$$

$$Ca_5(OH)(PO_4)_3(s) + F^- \rightarrow Ca_5F(PO_4)_3(s) + OH^- \quad (11)$$

Here $H_2PO_4^-$ (pK_{a2} = 7.21) dominates over HPO_4^{2-} (pK_{a3} = 12.35) in the pH range of treated water. The reactions of dissolution of $CaCO_3$ by the triprotic PA (pK_{a1} = 2.12), Eq. (5), the precipitation of CaF_2, Eq. (7) and the precipitation of FAP and HAP, Eqs. (8)–(10) are completed rapidly. Though FAP has a lower solubility product than that of HAP, a high abundance of hydroxide ion in the system makes precipitation of HAP more favourable. The sorption or exchange of the remaining fluoride by HAP, Eq. (11) continues for a longer time as indicated by the continued increase in fluoride removal till about an hour. Finally, it can be stated that defluoridation takes place predominantly through sorption of fluoride by HAP, formed in situ, in addition to the precipitation of CaF_2 and FAP.

3.6. Thermodynamics of adsorption

The thermodynamic parameters, viz., standard Gibb's free energy (ΔG^o), enthalpy change (ΔH^o) and change in entropy (ΔS^o), were determined from van't Hoff equation to understand the influence of temperature on fluoride adsorption by LSW (supporting information 5).

The calculated K_c values for the five different $[F^-]_0$ were plotted utilizing the van't Hoff equation. The values of standard enthalpy change (ΔH^o) and entropy change (ΔS^o) were acquired from the slope and intercept of the van't Hoff plot (Fig. 7) and presented in Table 5. Negative ΔG^o affirms the spontaneity of this fluoride removal process. In case of physical adsorption, ΔG^o ranges from –20 to 0 kJ mol^{-1} [51]. In the present study, the thermodynamic values obtained, are

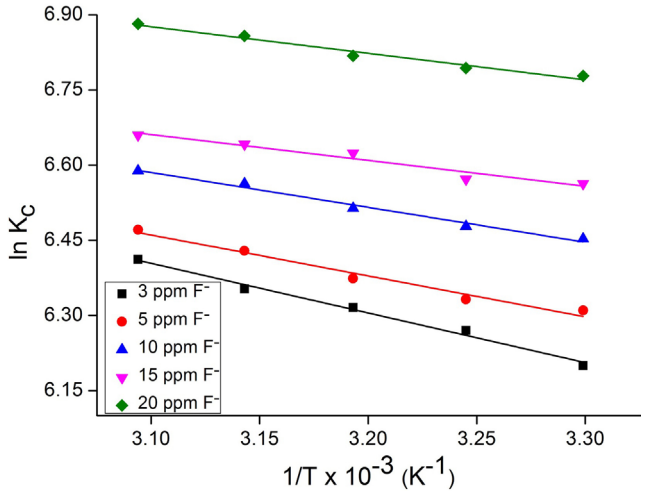

Fig. 7. The van't Hoff plot for fluoride adsorption on LSW at different $[F^-]_0$ in mg/L using 0.05 M $[PA]_0$ and sorbent dose of 1.5 g/100 mL.

within this range, thus confirming that the process is predominantly governed by physical adsorption. Positive values of ΔH^o and ΔS^o indicates endothermic adsorption and increasing randomness at the sorbent/solution interface, respectively.

3.7. Suitability analysis

3.7.1. Comparison of adsorption capacity

A comparison of the present adsorbent among other reported fluoride adsorbents, based on their adsorption capacities has been shown in supporting information 6. With an adsorption capacity of 0.943 mg g^{-1}, the present adsorbent was found to be better than that reported for adsorbents such as calcite (limestone), magnesite, laterite, gypsum, bauxite and limestone with PA. LSW was found to possess poorer adsorption capacity than certain adsorbents, viz., bauxite, clay, activated alumina, Al_2O_3/carbon nanotube, bone char, HAP, hydrothermally modified limestone, tamarind fruit-shell carbon and graphene. However, LSW has an advantage

Table 5
Thermodynamic parameters for adsorption of fluoride by the LSW

$[F^-]_0$ (mg/L)	ΔG^o (kJ mol^{-1})					ΔH^o (kJ mol^{-1})	ΔS^o (J K^{-1} mol^{-1})
	300 K	308 K	313 K	318 K	323 K		
3	–15.6	–16.1	–16.4	–16.8	–17.2	16.3	8.3
5	–15.9	–16.2	–16.6	–17.0	–17.4	18.1	8.5
10	–16.3	–16.6	–16.9	–17.4	–17.7	20.6	8.7
15	–16.5	–16.8	–17.2	–17.6	–17.9	23.1	8.9
20	–17.1	–17.4	–17.7	–18.1	–18.5	25.2	9.4

over the aluminium-containing materials, due to absence of leaching of aluminium, a suspect of Alzheimer's disease. Being an industrial waste with no economically viable methods for disposal or reuse, this fluoride adsorbent can gain an edge over the others in terms of cost, availability, acceptability by society and reusability.

3.7.2. Reusability of the sorbent

The reusability of the present sorbent for fluoride removal was examined by adding 3.75 g of fresh LSW to 250 mL pre-acidified water containing 5 mg/L $[F^-]_0$ and 0.05 M $[PA]_0$. The mixture was agitated at 140 rpm in a thermostat shaker for 90 min. The treated water was passed through ashless Whatman 42 filter paper and fluoride concentration in the treated water was measured. The filter paper was charred to recover the fluoride-loaded LSW which was again used to remove fluoride from identical fluoride spiked solutions. This process was repeated and fluoride concentrations in the treated water were measured each time. Results showed that the sorbent gradually lose its fluoride removal ability to 48% up to the 5th cycle, but then steeply deteriorated to 4% in the 6th cycle (Fig. 6(A)).

3.7.3. Disposal of exhausted sorbent

For the safe disposal of the used sorbent in the environment after repeated use, leaching of fluoride from the LSW was checked as per the toxicity characteristic leaching procedure (TCLP) test of the US-EPA [52]. Leaching of 0.034 mg/L was found from the sorbent, which is much lower than the permissible value of 150 mg/L for disposal in landfill [53].

4. Conclusions

The present study has shown that LSW from paper mill can efficiently remove fluoride in presence of phosphoric acid through precipitation and adsorption. Geochemical model PHREEQ has predicted the model pH and precipitation products in coherence with experimental observations. The PHREEQ predicted remaining fluoride in treated water has been found to be better than experimental results. Fluoride removal was achieved from initial 10 mg/L to less than 1 mg/L in 30 min. The final $[F^-]$ was found to decrease from 1.5 to 0.4 mg/L with decrease in initial $[F^-]$ from 20 to 3 mg/L. The final $[F^-]$ was also found to decrease with increase in adsorbent dose in the range of 5–35 g/L and increase in initial [PA] of 0.01–0.10 M. The observed 0.943 mg g^{-1} adsorption capacity of LSW is competitive among raw lime materials and there are scopes for improving the adsorption capacity through modification of LSW and scaling-up of the process. The adsorption data fitted well with Freundlich isotherm and pseudo-second-order kinetics. The adsorption process is spontaneous and endothermic in nature. Regarding safety and environmental consideration, while the relevant water quality parameters of the treated water conform to the WHO guideline, the exhausted used LSW very well passes the TCLP test of the US-EPA. Thus, the present study indicates that the waste material of LSW, when used in combination with dilute PA, has a great potential to make an efficient, environment-friendly and low-cost defluoridating agent for getting potable water as well as for treating industrial wastewater.

Acknowledgements

R. Mohan and A.J. Bora are thankful to Tezpur University for institutional fellowships. R.K. Dutta is thankful to the DST, New Delhi, for a research grant (DST/TM/WTI/2K16/95).

References

[1] A. Komarek, E. Lesaffre, T. Harkanen, D. Declerck, J.I. Virtanen, A Bayesian analysis of multivariate doubly-interval-censored dental data, Biostatistics, 6 (2005) 145–155.
[2] A.K. Susheela, A Treatise on Fluorosis, Fluorosis Research and Rural Development Foundation, New Delhi, 2001.
[3] WHO, Guideline for Drinking Water Quality, Recommendations, 4th ed., World Health Organization, Geneva, 2011.
[4] S. Ayoob, A.K. Gupta, V.T. Bhat, A conceptual overview on sustainable technologies for the defluoridation of drinking water, Crit. Rev. Environ. Sci. Technol., 38 (2008) 401–470.
[5] E.J. Reardon, Y. Wang, A limestone reactor for fluoride removal from wastewater, Environ. Sci. Technol., 34 (2000) 3247–3253.
[6] A. Bhatnagar, E. Kumar, M. Sillanpää, Fluoride removal from water by adsorption—a review, Chem. Eng. J., 171 (2011) 811–840.
[7] WHO, Fluorine and Fluorides, Environmental Health Criteria 36, World Health Organization, Geneva, 1984.
[8] W.G. Nawlakhe, D.N. Kulkarni, B.N. Pathak, K.R. Bulusu, Defluoridation using the Nalgonda technique in Tanzania, Ind. J. Environ. Health, 17 (1975) 26–65.
[9] S. Meenakshi, N. Viswanathan, Identification of selective ion-exchange resin for fluoride sorption, J. Colloid Interface Sci., 308 (2007) 438–450.
[10] J. Shen, A. Schafer, Removal of fluoride and uranium by nanofiltration and reverse osmosis: a review, Chemosphere, 117 (2014) 679–691.
[11] J. Lu, Q. Tang, Z.R. Wang, C. Xu, S.L. Lin, A study on continuous and batch electrocoagulation process for fluoride removal, Desal. Wat. Treat., 57 (2016) 28417–28425.
[12] A.B. Nasr, C. Charcosset, R.B. Amar, K. Walha, Defluoridation of water by nanofiltration, J. Fluorine Chem., 150 (2013) 92–97.

[13] A.A. Markeb, A. Alonso, A. Sánchez, X. Font, Adsorption process of fluoride from drinking water with magnetic core-shell Ce-Ti@Fe_3O_4 and Ce-Ti oxide nanoparticles, Sci. Total Environ., 598 (2017) 949–958.
[14] A. Maiti, J.K. Basu, S. De, Chemical treated laterite as promising fluoride adsorbent for aqueous system and kinetic modelling, Desalination, 265 (2011) 28–36.
[15] B.D. Turner, P. Binning, S.L.S. Stipp, Fluoride removal by calcite: evidence for fluoride precipitation and surface adsorption, Environ. Sci. Technol., 39 (2005) 9561–9568.
[16] S.K. Nath, R.K. Dutta, Fluoride removal from water using crushed limestone, Indian J. Chem. Technol., 17 (2010) 120–125.
[17] S.K. Nath, R.K. Dutta, Enhancement of limestone defluoridation of water by acetic and citric acids in fixed bed reactor, CLEAN Soil Air Water, 38 (2010) 614–622.
[18] S.K. Nath, R.K. Dutta, Acid-enhanced limestone defluoridation in column reactor using oxalic acid, Process Saf. Environ. Prot., 90 (2012) 65–75.
[19] S.K. Nath, R.K. Dutta, Significance of calcium containing materials for defluoridation of water: a review, Desal. Wat. Treat., 53 (2015) 2070–2085.
[20] B. Thole, F. Mtalo, W. Masamba, Groundwater defluoridation with raw bauxite, gypsum, magnesite, and their composites, CLEAN Soil Air Water, 40 (2012) 1222–1228.
[21] A. Salifu, B. Petrusevski, E.S. Mwampashi, I.A. Pazi, K. Ghebremichael, R. Buamah, C. Aubry, G.L. Amy, M.D. Kenedy, Defluoridation of groundwater using aluminum-coated bauxite: optimization of synthesis process conditions and equilibrium study, J. Environ. Manage., 181 (2016) 108–117.
[22] G. Asgari, B. Roshani, G. Ghanizadeh, The investigation of kinetic and isotherm of fluoride adsorption onto functionalize pumice stone, J. Hazard. Mater., 217 (2012) 123–132.
[23] E. Kır, H. Oruc, I. Kır, T. Sardohan-Koseoglu, Removal of fluoride from aqueous solution by natural and acid-activated diatomite and ignimbrite materials, Desal. Wat. Treat., 57 (2016) 21944–21956.
[24] S. Dobaradaran, M.A. Zazuli, M. Keshtkar, S. Noshadi, M. Khorsand, F.F. Ghasemi, V.N. Karbasdehi, L. Amiri, F. Soleimani, Biosorption of fluoride from aqueous phase onto *Padina sanctae crucis* algae: evaluation of biosorption kinetics and isotherms, Desal. Wat. Treat., 57 (2016) 28405–28416.
[25] S. Patil, S. Renukdas, N. Patel, Defluoridation of water using biosorbents: kinetic and thermodynamic study, Int. J. Res. Chem. Environ., 3 (2013) 125–135.
[26] V.K. Gupta, I. Ali, V.K. Saini, Defluoridation of wastewaters using waste carbon slurry, Water Res., 41 (2007) 3307–3316.
[27] B. Kemer, D. Ozdes, A. Gundogdu, V.N. Bulut, C. Duran, M. Soylak, Removal of fluoride ions from aqueous solution by waste mud, J. Hazard. Mater., 168 (2009) 888–894.
[28] R.K. Dutta, G. Saikia, B. Das, C. Bezbaruah, H.B. Das, S.N. Dube, Fluoride contamination in groundwater of central Assam, India, Asian J. Water Environ. Pollut., 3 (2006) 93–100.
[29] B. Das, J. Talukdar, S. Sarma, B. Gohain, R.K. Dutta, H.B. Das, S.C. Das, Fluoride and other inorganic constituents in groundwater of Guwahati, Assam, India, Curr. Sci., 85 (2003) 657–661.
[30] S. Meenakshi, R.C. Maheshwari, Fluoride in drinking water and its removal, J. Hazard. Mater., 137 (2006) 456–463.
[31] S. Deka, S. Yasmin, Utilization of lime sludge waste from paper mills for fish culture, Curr. Sci., 90 (2006) 1126–1130.
[32] D.L. Parkhurst, C.A.J. Appelo, User's Guide to PHREEQC (Version 2) - A Computer Program for Speciation, Batch Reaction, One-dimensional Transport, and Inverse Geochemical Calculations, U.S. Geological Survey Water-Resources Investigations Report 99–4259, USGS, Denver, CO, 1999.
[33] S. Gogoi, R.K. Dutta, Fluoride removal by hydrothermally modified limestone powder using phosphoric acid, J. Environ. Chem. Eng., 4 (2016) 1040–1049.
[34] Y. Wang, N. Chen, W. Wei, J. Cui, Z. Wei, Enhanced adsorption of fluoride from aqueous solution onto nanosized hydroxyapatite by low-molecular-weight organic acids, Desalination, 276 (2011) 161–168.
[35] M. Hariharan, N. Varghese, A.B. Cherian, P.V. Sreenivasan, J. Paul, A. Antony, Synthesis and characterisation of $CaCO_3$ (calcite) nano particles from cockle shells using chitosan as precursor, Int. J. Sci. Res. Publ., 4 (2014) 1–5.
[36] A. Amalraj, A. Pius, Removal of fluoride from drinking water using aluminium hydroxide coated activated carbon prepared from bark of *Morinda tinctoria*, Appl. Water Sci., 7 (2017) 2653–2665.
[37] S. Gogoi, R.K. Dutta, Mechanism of fluoride removal by phosphoric acid-enhanced limestone: equilibrium and kinetics of fluoride sorption, Desal. Wat. Treat., 57 (2015) 6838–6851.
[38] S. Mandel, A.C. Tas, Brushite ($CaHPO_4{\cdot}2H_2O$) to octacalcium phosphate ($Ca_8(HPO_4)_2(PO_4)_4{\cdot}5H_2O$) transformation in DMEM solutions at 36.5°C, Mater. Sci. Eng., C, 30 (2010) 245–254.
[39] M.M. Khunur, A. Risdianto, S. Mutrofin, Y.P. Prananto, Synthesis of fluorite (CaF_2) crystal from gypsum waste of phosphoric acid factory in silica gel, Bull. Chem. Eng. Catal., 7 (2012) 71–77.
[40] D.J. Michalak, S.R. Amy, D. Aureau, M. Dai, A. Estève, Y.J. Chabal, Nanopatterning Si(111) surfaces as a selective surface-chemistry route, Nat. Mater., 9 (2010) 266–271.
[41] G.E.J. Poinern, M.K. Ghosh, Y.J. Ng, T.B. Issa, S. Anand, P. Singh, Defluoridation behavior of nanostructured hydroxyapatite synthesized through an ultrasonic and microwave combined technique, J. Hazard. Mater., 185 (2011) 29–37.
[42] C.S. Sundaram, N. Viswanathan, S. Meenakshi, Defluoridation chemistry of synthetic hydroxyapatite at nano scale: equilibrium and kinetic studies, J. Hazard. Mater., 155 (2008) 206–215.
[43] T.S.B. Narasaraju, U.S. Rai, Some thermodynamic aspects of dissolution of solid solutions of hydroxylapatites of phosphorus and arsenic, Can. J. Chem., 57 (1979) 2662.
[44] R. Aldaco, A. Garea, A. Irabien, Fluoride recovery in a fluidized bed: crystallization of calcium fluoride on silica sand, Ind. Eng. Chem. Res., 45 (2006) 796–802.
[45] X. Guo, W. Wang, G. Wu, J. Zhang, C. Mao, Y. Deng, H. Xia, Controlled synthesis of hydroxyapatite crystals template by novel surfactants and their enhanced bioactivity, New J. Chem., 35 (2011) 663–671.
[46] Standard Methods for the Examination of Water and Wastewater, American Public Health Association (APHA), New York, 1998.
[47] W. Nigussie, F. Zewge, B.S. Chandravanshi, Removal of excess fluoride from water using waste residue from alum manufacturing process, J. Hazard. Mater., 147 (2007) 954–963.
[48] S. Gogoi, S.K. Nath, S. Bordoloi, R.K. Dutta, Fluoride removal from groundwater by limestone treatment in presence of phosphoric acid, J. Environ. Manage., 152 (2015) 132–139.
[49] Y.S. Ho, G. McKay, A comparison of chemisorption kinetic models applied to pollutant removal on various sorbents, Process Saf. Environ. Prot., 76 (1998) 332–340.
[50] V. Sivasankar, S. Rajkumar, S. Murugesh, A. Darchen, Influence of shaking or stirring dynamic methods in the defluoridation behavior of activated tamarind fruit shell carbon, Chem. Eng. J., 197 (2012) 162–172.
[51] M.J. Jaycock, G.D. Parfitt, Chemistry of Interfaces, Ellis Horwood Onichester, 1981.
[52] Method 1311, Toxicity Characteristic Leaching Procedure, U.S. Environmental Protection Agency (USEPA), Washington, D.C., 1992.
[53] G. Bongo, G. Mercier, M. Chartier, A. Dhenain, J. Blais, Treatment of aluminium plant hazardous wastes containing fluoride and PAH, J. Environ. Eng., 135 (2009) 159–166.

Supporting information

Supporting information 1

Pictures of the menace created by dumping lime sludge waste (LSW) by Nagaon Paper Mill in Assam, India (Figs. S1 and S2).

Supporting information 2

Adsorption capacity of LSW and pure SiO_2 in different ratios (Fig. S3).

Supporting information 3

Results of pseudo-first-order, intra-particle diffusion and Elovich model adsorption kinetics study of fluoride by LSW.

Pseudo-first-order model

The pseudo-first-order equation for sorption of liquid/solid systems based on solid capacity can be represented as follows [1]:

$$\ln\left(q_e - q_t\right) = \ln q_e - k_1 t \tag{1}$$

where q_e and q_t are the amount of solute on the surface of the sorbent in mg g^{-1} at equilibrium and at time t, respectively, and k_1 is the pseudo-first-order rate constant in min^{-1}. k_1 and the theoretical defluoridation capacity of the sorbent (q_e, cal) were calculated from the plot of ln ($q_e - q_t$) vs. time t (Fig. S4). The squared correlation coefficients (r^2) of this model were found to be between 0.839 and 0.951 with minimal similarity between the calculated q_e and experimental q_e values predicting that the sorption data do not fit well to the pseudo-first-order model.

Fig. S1. A picture of the dumping site of LSW in front of Nagaon Paper Mill, Jagiroad, Assam, India.

Fig. S2. A google map of the paper mill and the LSW dumping sites located near Jagiroad, Assam, India (Coordinates: 26.125813, 92.21739).

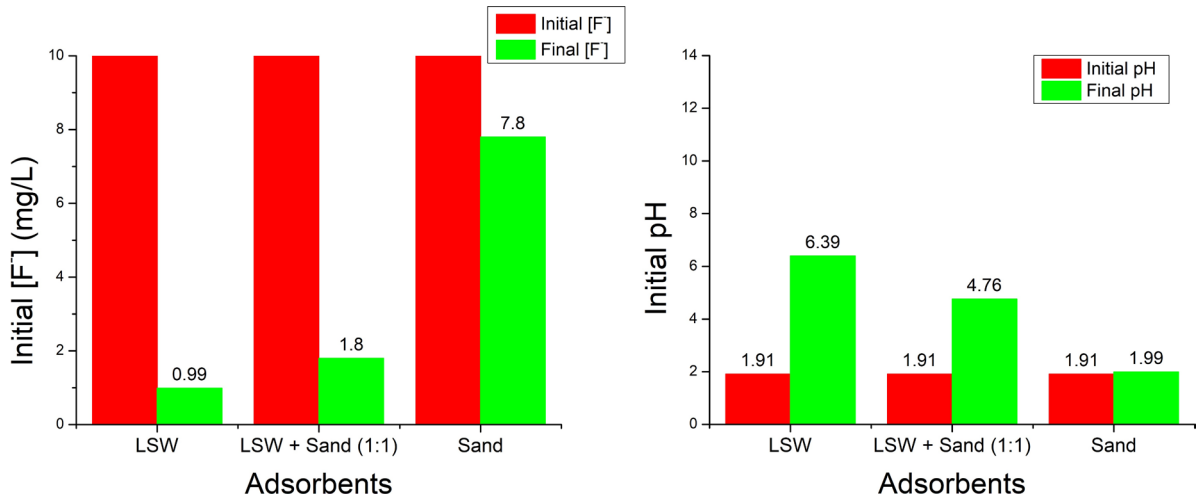

Fig. S3. Comparison between the adsorption capacity of LSW and pure SiO_2 in different ratios experimental conditions: initial pH: 1.85, temperature = 300 K, $[F]_0$ = 10 mg/L, $[PA]_0$ = 0.05 M, adsorbent dose: 1.5 g/100 mL, contact time = 90 min and agitation speed = 140 rpm.

Intra-particle diffusion model

Using the intra-particle diffusion model, the initial rate of intra-particle diffusion can be calculated using the equation given below [2]:

$$q_t = k_i t^{1/2} + C \tag{2}$$

where q_t and k_i are the amount of fluoride adsorbed by the sorbent at time t and intra-particle diffusion rate constant in mg g^{-1} $min^{-1/2}$, respectively. C in mg/g gives an impression about the thickness of boundary layer. The graph of q_t vs. $t^{1/2}$ for intra-particle diffusion model was plotted (Fig. S5) and k_i was calculated from the slope of this graph. The r^2 values are unsatisfactory indicating the inapplicability of this model for determining the kinetics of the process. In addition, the curves in this plot did not pass through the origin implying that the mechanism of fluoride removal by LSW is not solely controlled by intra-particle diffusion. The increasing values of k_i with increasing $[F^-]_0$ indicates intra-particle diffusion to be concentration dependent for this adsorption process [3].

Elovich model

The linear form of Elovich model can be presented as follows [4]:

$$q_t = \left(\frac{1}{B}\right)\ln AB + \left(\frac{1}{B}\right)\ln t \tag{3}$$

where A in mg g^{-1} min^{-1} and B in g mg^{-1} are the sorption and desorption constants of fluoride ions for distinct trials. The values of A and $1/B$ were obtained from the plot of q_t vs. ln t (Fig. S6). The r^2 values are better than that of intra-particle diffusion model suggesting the relevance of this model. With increasing initial $[F^-]_0$, the desorption constant ($1/B$) values were found to increase from 0.0120 to 0.0979 mg g^{-1} indicating a decrease in number of available active sites for fluoride adsorption with increase in initial fluoride concentration.

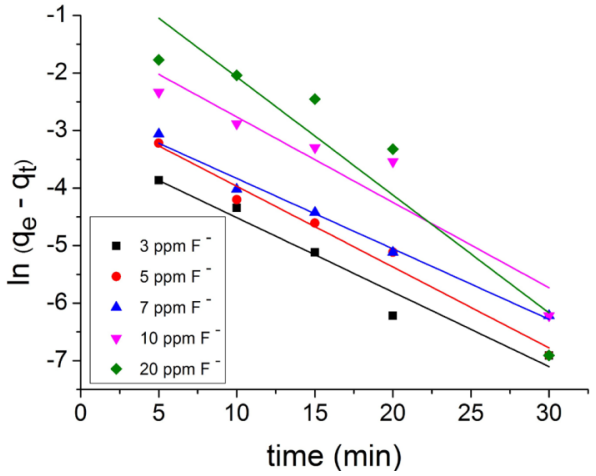

Fig. S4. Pseudo-first-order plot at different $[F^-]_0$ in mg/L using 0.05 M PA and adsorbent dose of 1.5 g/100 mL at 300 (±1) K.

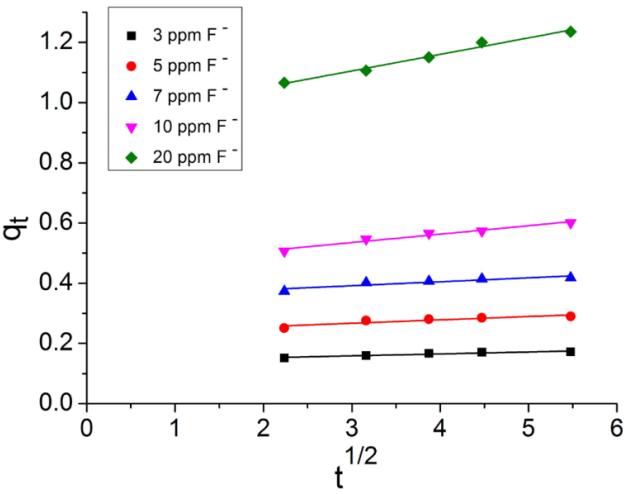

Fig. S5. Intra-particle diffusion plot at different $[F^-]_0$ in mg/L using 0.05 M PA and adsorbent dose of 1.5 g/100 mL at 300 (±1) K.

Supporting information 4

Results of the study of Langmuir, Temkin and Dubinin–Radushkevich (D–R) adsorption isotherms:

Langmuir isotherm

Langmuir isotherm can be represented by the linear equation as below [1]:

$$\frac{C_e}{q_e} = \frac{C_e}{Q_o} + \frac{1}{bQ_o} \tag{4}$$

where b in L mg^{-1} and Q_o in mg g^{-1} are the Langmuir isotherm constants and are related to adsorption energy and adsorption capacity, respectively [5]. The value of Q_o and b are obtained from the slope and intercept of the plot of C_e/q_e vs. C_e (Fig. S7). The value of r^2 for the Langmuir plot is poorer than the Freundlich plot indicating the adsorption to be essentially physisorption.

The feasibility of Langmuir isotherm can be calculated in terms of a dimensionless constant separation factor R_L which can be represented by the equation given below [6,7]:

$$R_L = \frac{1}{1 + bC_o} \tag{5}$$

where R_L is a dimensionless equilibrium parameter and C_o is the initial fluoride concentration. The observed R_L values between 0 and 1 suggest a favoured Langmuir adsorption (Table S1) [6].

Temkin isotherm

The linear form of Temkin isotherm can be expressed as follows [8]:

$$q_e = B_T\left(\ln A_T + \ln C_e\right) \tag{6}$$

where $B_T = (RT)/b$ and A_T in L/g are Temkin constants. The value of B_T and A_T is obtained from the slope and intercept of the plot of q_e vs. ln C_e (Fig. S8). The observed poor r^2 value suggests that this model cannot describe the mechanism of fluoride adsorption appropriately. From the low value of B_T, it can be inferred that there is a favourable lower heat of exchange of OH^- ions of the HAP formed, by F^- ions [9].

Dubinin–Radushkevich isotherm

The D–R isotherm is more general than the Langmuir isotherm and helps in having a superior grasp on the type of adsorption from the amount of fluoride both in the sorbent and solution at equilibrium [5]. The linear form of D–R equation is given below:

$$\ln q_e = \ln Q_D - B_D\varepsilon^2 \tag{7}$$

where Q_D is the maximum theoretical adsorption capacity in mg g^{-1}, B_D is D–R model constant in mol^2 kJ^{-2} related to mean sorption energy and ε is the Polanyi potential. The value of Q_D and B_D is derived from the slope and intercept of the plots of (ln q_e) vs. ε^2 (Fig. S9).

For information about the type of adsorption, the magnitude of mean free energy of adsorption E is determined using the equation given below [10]:

$$E = \left(2B_D\right)^{-0.5} \tag{8}$$

Table S1
Values of R_L at different $[F^-]_0$ for the sorbent

$[F^-]_0$ (mg/L)	R_L
3	0.206
5	0.135
7	0.100
10	0.072
20	0.037

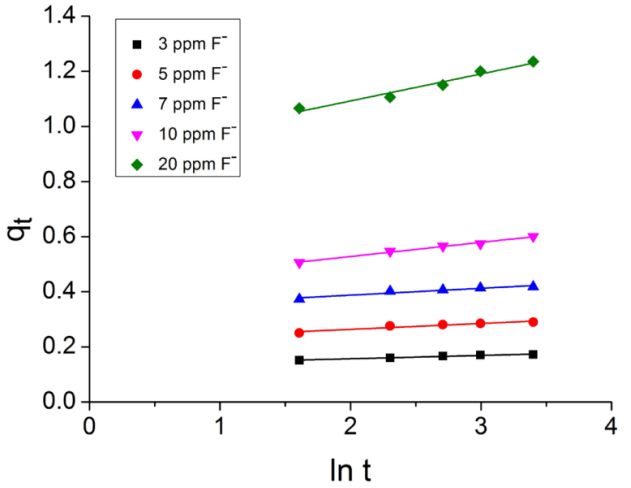

Fig. S6. Elovich plot at different $[F^-]_0$ in mg/L using 0.05 M PA and adsorbent dose of 1.5 g/100 mL at 300 (±1) K.

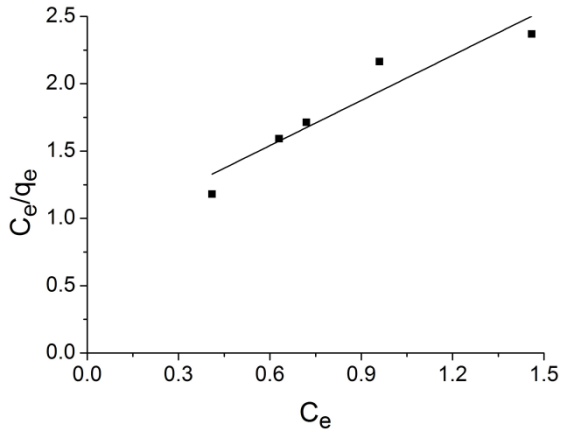

Fig. S7. Plot of Langmuir isotherm for fluoride sorption on LSW at varying $[F^-]_0$ of 3, 5, 7, 10 and 20 mg/L with a sorbent dose of 1.5 g/100 mL and $[PA]_0$ of 0.05 M at 300 (±1) K.

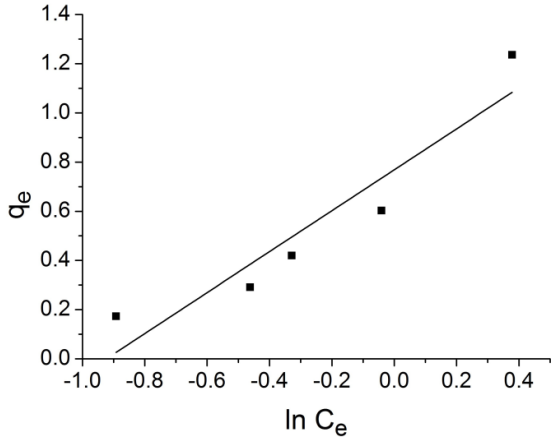

Fig. S8. Plot of Temkin isotherm for fluoride sorption on LSW at varying $[F^-]_0$ of 3, 5, 7, 10 and 20 mg/L with a sorbent dose of 1.5 g/100 mL and $[PA]_0$ of 0.05 M at 300 (±1) K.

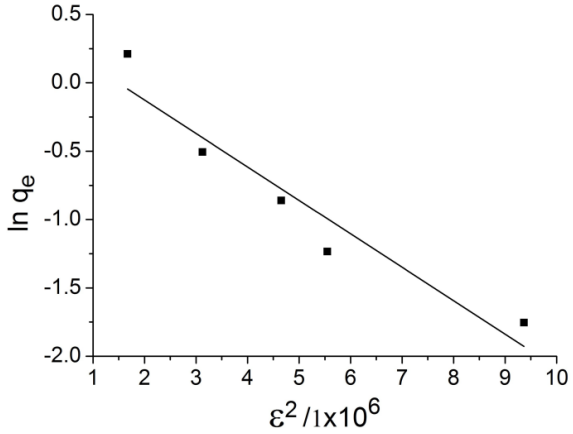

Fig. S9. Plot of D–R isotherm for fluoride sorption on LSW at varying $[F^-]_0$ of 3, 5, 7, 10 and 20 mg/L with a sorbent dose of 1.5 g/100 mL and $[PA]_0$ of 0.05 M at 300 (±1) K.

The value of E has been found to be less than 8 kJ mol^{-1}, thus again indicating the fluoride adsorption to be governed predominantly by physical adsorption [11]. The r^2 value is better than that of Langmuir and Temkin isotherms suggesting that the D–R isotherm befits the adsorption process.

Supporting information 5

The van't Hoff plot of fluoride adsorption on LSW

The thermodynamic parameters, viz., standard Gibb's free energy (ΔG^o), enthalpy change (ΔH^o) and change in entropy (ΔS^o) were calculated using the following relationships:

$$\Delta G^o = -RT \ln K_c \tag{9}$$

$$\Delta G^o = \Delta H^o - T\Delta S^o \tag{10}$$

$$\ln K_c = \frac{\Delta S^o}{R} - \frac{\Delta H^o}{RT} \tag{11}$$

Table S2
Comparison of adsorption capacity of the present adsorbent with various reported adsorbents

Adsorbent	Capacity (mg g^{-1})	Reference
Calcite	0.39	[12]
Magnesite	0.71	[13]
Gypsum	0.85	[13]
Laterite	0.86	[13]
Lime sludge waste with PA	0.94	This work
Bauxite	1.05	[13]
Limestone with PA	1.10	[14]
Clays	1.69	[15]
Activated alumina	2.41	[16]
Bone char	2.50	[17]
HAP	4.54	[12]
Nano-HAP	5.50	[1]
Hydrothermally modified limestone	6.45	[9]
Brushite	6.59	[10]
Al_2O_3/carbon nanotube	13.5	[18]
Tamarind fruit-shell carbon	22.33	[19]
Graphene	41	[20]

where R is the universal gas constant, T is the temperature in Kelvin and K_c is the equilibrium constant, which is generally expressed as:

$$K_c = \frac{q_e}{C_e} \tag{12}$$

Supporting information 6

Comparison of adsorption capacity is shown in Table S2.

References

[1] G.E.J. Poinern, M.K. Ghosh, Y.J. Ng, T.B. Issa, S. Anand, P. Singh, Defluoridation behavior of nanostructured hydroxyapatite synthesized through an ultrasonic and microwave combined technique, J. Hazard. Mater., 185 (2011) 29–37.
[2] W.J. Weber, J.C. Morris, Equilibria and capacities for adsorption on carbon, J. Sanit. Eng. Div., 90 (1964) 79–107.
[3] M. Islam, P.C. Mishra, R. Patel, Physicochemical characterization of hydroxyapatite and its application towards removal of nitrate from water, J. Environ. Manage., 91 (2010) 1883–1891.
[4] C. Aharoni, F.C. Tompkins, Kinetics of adsorption and desorption and the Elovich equation, Adv. Catal., 21 (1970) 1–49.
[5] A. Amalraj, A. Pius, Removal of fluoride from drinking water using aluminium hydroxide coated activated carbon prepared from bark of *Morinda tinctoria*, Appl. Water Sci., 7 (2017) 2653–2665.
[6] Y. Wang, N. Chen, W. Wei, J. Cui, Z. Wei, Enhanced adsorption of fluoride from aqueous solution onto nanosized hydroxyapatite by low-molecular-weight organic acids, Desalination, 276 (2011) 161–168.
[7] T.W. Weber, R.K. Chakravorti, Pore and solid diffusion models for fixed bed adsorbers, AlChE J., 20 (1974) 228–238.

[8] M.I. Temkin, V. Pyzhev, Kinetics of ammonia synthesis on promoted iron catalysts, Acta Physiochim. URSS, 12 (1940) 327–356.
[9] S. Gogoi, R.K. Dutta, Fluoride removal by hydrothermally modified limestone powder using phosphoric acid, J. Environ. Chem. Eng., 4 (2016) 1040–1049.
[10] M. Mourabet, H. El Boujaady, A. El Rhilassi, H. Ramdane, M. Bennani-Ziatni, R. El Hamri, A. Taitai, Defluoridation of water using brushite: equilibrium, kinetic and thermodynamic studies, Desalination, 278 (2011) 1–9.
[11] W. Nigussie, F. Zewge, B.S. Chandravanshi, Removal of excess fluoride from water using waste residue from alum manufacturing process, J. Hazard. Mater., 147 (2007) 954–963.
[12] X. Fan, D.J. Parker, M.D. Smith, Adsorption kinetics of fluoride on low cost materials, Water Res., 37 (2003) 4929–4937.
[13] B. Thole, F. Mtalo, W. Masamba, Groundwater defluoridation with raw bauxite, gypsum, magnesite, and their composites, CLEAN Soil Air Water, 40 (2012) 1222–1228.
[14] S. Gogoi, S.K. Nath, S. Bordoloi, R.K. Dutta, Fluoride removal from groundwater by limestone treatment in presence of phosphoric acid, J. Environ. Manage., 152 (2015) 132–139.
[15] A.D. Atasoy, M.O. Sahin, Adsorption of fluoride on the raw and modified cement clay, CLEAN Soil, Air, Water, 42 (2014) 415–420.
[16] S. Ghorai, K.K. Pant, Equilibrium kinetics and breakthrough studies for adsorption of fluoride on activated alumina, Sep. Purif. Technol., 42 (2005) 265–271.
[17] D.L. Mawaniki, J.M. Simwa, F. Manji, Fluoride binding capacity of bone charcoal and its effects on selected micro-organisms, East Afr. Med. J., 67 (1990) 427–431.
[18] Y.H. Li, S. Wang, A. Cao, D. Zhao, X. Zhang, C. Xu, Z. Luan, D. Ruan, J. Liang, D. Wu, B. Wei, Adsorption of fluoride from water by amorphous alumina supported on carbon nanotubes, Chem. Phys. Lett., 350 (2001) 412–416.
[19] V. Sivasankar, S. Rajkumar, S. Murugesh, A. Darchen, Tamarind (*Tamarindus indica*) fruit shell carbon: a calcium-rich promising adsorbent for fluoride removal from groundwater, J. Hazard. Mater., 225 (2012) 164–172.
[20] Y. Li, P. Zhang, Q. Du, X. Peng, T. Liu, Z. Wang, Y. Xia, W. Zhang, K. Wang, H. Zhu, D. Wu, Adsorption of fluoride from aqueous solution by graphene, J. Colloid Interface Sci., 363 (2011) 348–354.